Accepted Manuscript

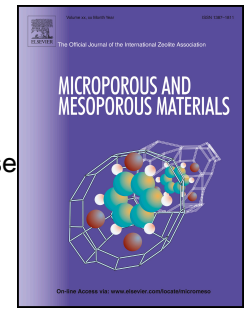

Surface-functionalization of mesoporous SBA-15 silica materials for controlled release of methylprednisolone sodium hemisuccinate: Influence of functionality type and strategies of incorporation

J. Ortiz-Bustos, A. Martín, V. Morales, R. Sanz, R.A. García-Muñoz

PII: S1387-1811(16)30543-1

DOI: 10.1016/j.micromeso.2016.11.021

Reference: MICMAT 8013

To appear in: *Microporous and Mesoporous Materials*

Received Date: 8 February 2016

Revised Date: 6 October 2016

Accepted Date: 22 November 2016

Please cite this article as: J. Ortiz-Bustos, A. Martín, V. Morales, R. Sanz, R.A. García-Muñoz, Surface-functionalization of mesoporous SBA-15 silica materials for controlled release of methylprednisolone sodium hemisuccinate: Influence of functionality type and strategies of incorporation, *Microporous and Mesoporous Materials* (2016), doi: 10.1016/j.micromeso.2016.11.021.

Surface-functionalization of mesoporous SBA-15 silica materials for controlled release of methylprednisolone sodium hemisuccinate: influence of functionality type and strategies of incorporation

J. Ortiz-Bustos, A. Martín, V. Morales, R. Sanz, and R. A. García-Muñoz

Chemical and Environmental Engineering Group, Universidad Rey Juan Carlos, C/ Tulipán s/n, 28933 Móstoles, Madrid, Spain

Graphical Abstract

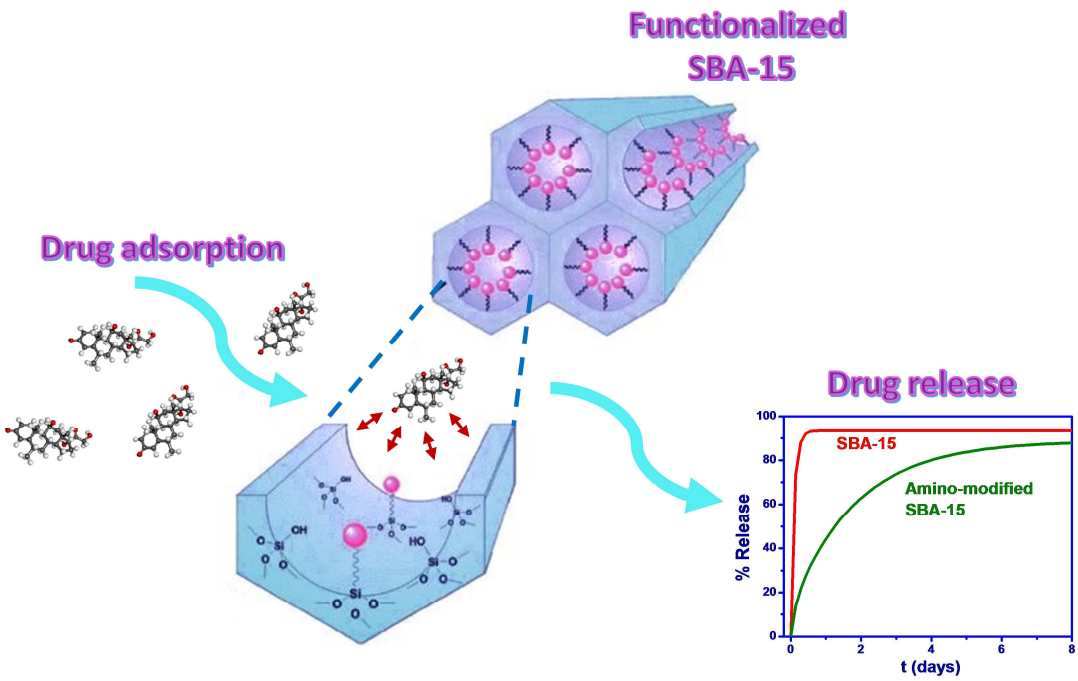

Surface-functionalization of mesoporous SBA-15 silica materials for controlled release of methylprednisolone sodium hemisuccinate: influence of functionality type and strategies of incorporation

J. Ortiz-Bustos, A. Martín, V. Morales, R. Sanz, and R. A. García-Muñoz

Chemical and Environmental Engineering Group, Universidad Rey Juan Carlos,

C/ Tulipán s/n, 28933 Móstoles, Madrid, Spain

Abstract

Mesoporous SBA-15 silica materials functionalized with several organic moieties, that include different polarities and hydrophobicities, were investigated as matrices for controlled drug delivery. The functionalities were incorporated into SBA-15 using two methods: direct synthesis or co-condensation route and post-synthesis grafting. Methylprednisolone sodium hemisuccinate, a synthetic pharmaceutical compound used as anti-inflammatory and immunosuppressant, was loaded onto the pristine and functionalized mesoporous SBA-15 silica materials. The influence of the type of organic moieties as well as their incorporation method onto the inorganic silica framework has been evaluated. The results show that SBA-15 functionalized with aminopropyl trimethoxysilane groups has the largest capacity of drug adsorption, clearly higher than the provided by materials functionalized with other groups, independently of the synthesis route. Additionally, materials synthesized by the co-condensation approach show a lower degree of drug retention than the same material synthesized by grafting technique. This fact is attributed to the distinct localization of the functionality, more accessible in the case of the grafting procedure, and hence suggesting that stronger interactions among the SBA-15 functionalized surfaces and the model drug are established. To ascertain whether other organosilanes containing amino groups can provide more effective loading and controlled drug delivery, at neutral and acidic conditions (pH of 7.4 and 4.6, respectively), it was also investigated the incorporation by grafting of several amino organic moieties onto the SBA-15 silica materials. It was concluded that as the number of amino groups incorporated into SBA-15

material increased, not only the drug loading capacity was higher, but the functionalized silica material vehicles slowed down the drug delivery. Finally, it was confirmed that cell viability was largely unaffected by amino-functionalized mesoporous SBA-15 silica materials after 72 h of incubation time.

Keywords: SBA-15, surface modification, methylprednisolone, drug release.

1. Introduction

Mesostructured silica particles have been widely applied in the areas of catalysis, adsorption and separation processes [1]. More recently, these ordered mesoporous materials have been used also as matrices in controlled drug delivery systems [2-5] due to their high specific surface areas, tuneable pore sizes, good biocompatibility and facile surface functionalization. In particular, SBA-15 has been one of the most extensively studied ordered mesoporous materials due to its chemical, thermal and mechanical stability together with a highly ordered hexagonal topology and large pore size [6-10]. However, the pure silica materials only have non-condensed silanol groups on the channel walls that involve a weak intermolecular hydrogen bonding with the most of organic groups, providing low capacity of drug adsorption. Hence, the application of SBA-15 mesoporous silica as carriers in controlled drug delivery systems (DDS) is limited. A likely solution to circumvent this drawback consists of modifying the surface of mesoporous materials by means of functionalized organosilanes [11]. Thus, the interactions between modified silica carrier and adsorbed drug may influence the degree of drug loading and release. Numerous functionalities have been incorporated into mesoporous materials with the objective of modifying the chemical properties of the surfaces. Surface modification of mesoporous matrices can generate, among other, acid [12-14] or basic [15, 16] character, surface hydrophobization [17], thermoresponsive properties [18] optical properties induction [19] and photocatalytic activity [20]. Another recently approach, recently reported, to increase the applications of the mesostructured silica materials as DDS is based on the design of drug-structure-directing agent with dual inherent pharmacological activity and ability to direct the

formation of solid and hollow-shell MSNs. [21]. Direct synthesis (co-condensation) and post-synthesis (grafting) procedures are the two main approaches used in functionalization of mesoporous materials. Direct synthesis method consists in the co-condensation of tetraalkoxysilanes with terminal trialkoxyorganosilanes in the presence of structure-directing agents. Since organosilane functionalities are sources of silica, mesoporous materials with homogeneously distributed functional groups are prepared by this method [22-24]. Moreover, a good control over surface properties of the resultant material is provided [25]. However, certain drawbacks are associated with co-condensation method such as the decrease of the degree of mesoscopic order with increasing concentration of organic groups [26], or that a high fraction of the functional groups are inaccessible and embedded in the silica network. Post-synthesis grafting route is based on the reaction between an organoalkoxysilane precursor of the organic chain and the silanol groups of the silica support [27]. This method of functionalization has the advantage that the mesostructure of the starting silica phase is usually retained [28]. In addition, the accessibility to the loaded organic moieties is high since the reaction of organosilane species with the silanol groups takes place at the silica surface. Nevertheless, certain drawbacks are also associated with post-synthesis grafting method. Thus, this method usually results in heterogeneous surface coverage due to preferential organic moieties aggregation near the entries of the mesopores and the outer surface of the particles [29]. In addition, a restricted amount of functional groups can be grafted because of the limited density of silanol groups at the reactive surface [30].

The corticosteroid methylprednisolone sodium hemisuccinate is a synthetic drug that has been used since several decades as an anti-inflammatory or immunosuppressant agent for the treatment of hematologic, allergic, inflammatory, neoplastic, and autoimmune origin diseases [31]. However, this steroid drug has not been extensively studied to date as formulations involving the use of modified mesoporous silica materials. For these, nonsteroidal ibuprofen has long been the drug molecule of choice when investigating surface modifying agent, while

pharmaceutical anticancer agents have been the cargo under study when investigating the drug delivery capability either in vitro or in vivo [32, 33].

Thus, the objective of this paper was to modify the surface of inorganic mesoporous SBA-15 silica materials with several functionalities of different chemical nature using the direct synthesis (co-condensation) route and the post-synthesis grafting method. The amount of organosilane moieties incorporated onto the silica was evaluated using elemental and thermogravimetric analyses, while the textural properties of materials were determined from N_2 adsorption analyses. A model steroidal drug, methylprednisolone hemisuccinate, was selected to load onto the SBA-15 functionalized silica materials and *in vitro* release in aqueous biological media at neutral and acidic conditions were carried out. Zeta potential values for modified silica materials were measured to determine the electrostatic interactions among pharmaceutical methylprednisolone hemisuccinate and the modified silica surface. The release rates of methylprednisolone from functionalized mesoporous silica into simulated body fluids were correlated with the organosilane functionalities decorating the surface of the SBA-15 and also with their incorporation strategy onto the silica.

2. Experimental

2.1 Synthesis of pure silica SBA-15 and organically-modified mesoporous materials

Synthesis of pure SBA-15 was performed according to a previously described method [34]. Usually, 4 g of the structure-directing agent - block-copolymer Pluronic 123 ($EO_{20}PO_{70}EO_{20}$) were dissolved under stirring in 1.9 M HCl (125 mL) at room temperature. The resultant micellar solution was then heated to 40 ºC before adding 8 g of the silica source, tetraethylorthosilicate (TEOS). The mixture was stirred at 100 °C for 24 h under static conditions. Thereafter, the solid product was recovered by filtration, washed with deionized water and dried at 60 °C overnight. The surfactant template was removed following two different methods: a) by calcination at 550 ºC for 5 h with a heating rate of 1.8 ºC·min^{-1} (SBA-15-cal) or b) by refluxing with ethanol for 24 h (SBA-15-ext).

Functionalized SBA-15 samples prepared by co-condensation method were carried out using the same procedure as that used in the synthesis of pure silica SBA-15 material except for adding a certain amount of selected organosilanes 1 h after adding the silica source (TEOS). In this case, the surfactant template was removed by refluxing with ethanol (1 g of sample in 100 mL of ethanol) for 24 h.

Prior to the functionalization process by grafting, and in order to increase the number of surface silanol groups, a rehydroxylation process was carried out by refluxing the calcined SBA-15 silica sample in hydrochloric acid (18.5 % w/w) for 12h. Subsequently, the re-hydroxylated SBA-15 silica was carefully vacuum-dried. This method has previously been shown to lead to an increase in the surface silanol concentration from 2 to 5 $\mu mol \cdot m^2$ for mesoporous MCM materials [35] and SBA-15 materials [36], without observing loss of mesoscopic order for the treated samples. Afterwards, the different functionalities were incorporated using a post-synthesis grafting method consists of the reaction between the re-hydroxylated SBA-15 material and the corresponding organosilane, under nitrogen, with anhydrous toluene and stirring at 60 ºC for 24 h. The resulting solid was filtered, washed with toluene to remove the excess of non-reacted organosilane and dried under vacuum at room temperature overnight.

The organosilanes used as functionalizing agents for both co-condensation and grafting processes were 3-(aminopropyl)trimethoxysilane (AP), 2-(4-chlorosulfonylphenyl)ethyltrimethoxysilane (AS), 3-(mercaptopropyl)trimethoxysilane (MP), chlorotrimethylsilane (TM), styrylethyltrimethoxysilane (ES), trimethoxy(octyl)silane (OC), 1-naphthyltrimethoxysilane (NF), *N*-(3-trimethoxysilylpropyl)ethylenediamine (ED), *N*-(3-trimethoxysilylpropyl)diethylenetriamine (DT), (*N*-phenylaminopropyl)trimethoxysilane (PAP) and (aminoethylaminomethyl)phenethyltrimethoxysilane (AEMP3) (Scheme 1). All of them were incorporated using an organosilane/TEOS molar ratio of 1/9. This value was selected in base to previous works to avoid, in the case of materials synthesized using co-condensation method, the usual disorder pore structure caused by high organosilane amount, and in the case of grafting route, the low incorporation organic yield due to the limited density of free silanol groups [5].

Functionalized mesoporous silica materials were denoted as AP-SBA-15, AS-SBA-15, MP-SBA-15, TM-SBA-15, SE-SBA-15, OC-SBA-15, NF-SBA-15, ED-SBA-15, DT-SBA-15, PAP-SBA-15 and AEMP3-SBA-15 in the forthcoming text. To distinguish between direct synthesis (co-condensation) and grafting, the supports were designated with a –C or –G final, respectively.

Scheme 1

2.2 Drug loading

Methylprednisolone hemisuccinate was loaded into the synthesized materials by the solvent adsorption method from a highly concentrated solution of the drug. SBA-15 or the functionalized materials (0.1 g) were added to a solution of methylprednisolone hemisuccinate (150 mg) in water (10 mL). This suspension was stirred at 260 rpm over 24 h at 25 ^{o}C while the evaporation of solvent was prevented in a sealed glass tube. The suspension was centrifuged at 3500 rpm over 10 minutes after which the supernatant was separated and the impregnated solids were dried overnight at 70 ^{o}C in a vacuum oven.

The determination of the methylprednisolone hemisuccinate loading was measured spectrophotometrically at a wavelength of 247 nm in a UV-Spectrometer (JASCO V-630) by the difference between the initial concentration and the concentration of drug in the supernatant.

2.3 Drug release studies

Sterilized dialysis bags with dialyzer-weight cut-off 10,000 Da were used to carry out the drug release experiments, although they were pre-treated prior to use as follows. The dialysis bags were fully immersed into 50 % aqueous solution of ethanol at 40 ^{o}C over 1h, and then washed with water up to 40 ^{o}C for one hour more. Finally, the dialysis bags were immersed in 100 mL of the simulated body fluid for 2h in order to stabilize them. This simulated medium was Phosphate Buffered Saline (PBS) of 7.4 pH and Acetate Buffered Solution of 4.65 pH, used as

the drug release media to simulate normal blood/tissues and acidic environment, respectively [37].

The drug-adsorbed samples (0.05 g) were placed into pretreated dialysis bags with 2 mL of release media. The sealed dialysis bags were put into glass bottles and then 100 mL of release media was added. The solution was shaken at 100 rpm at 37 ^{o}C under a sealed condition. The concentration of the released drug was calculated using the Lambert-Beer law according to the absorbance of the release media at 247 nm, which is the characteristic adsorption wavelength for the methylprednisolone hemisuccinate molecule. UV-Spectrometry (JASCO V-630) was the analytical method used for monitoring the amount of drug released as a function of time.

2.4 Cell culture and viability Assay

Breast cancer cells MDA-MB-231 were seeded at 30 % confluence, in DMEM (Dubelcco Modified Eagle's Medium) supplemented with 10% fetal calf serum, 2 mM L-glutamine, 100 U mL^{-1} penicillin, 100 μg·mL^{-1} streptomycin at 37 ° C in a 5 % CO_2 / 95% O_2 and 90 % RH humidify atmosphere.

MDA-MB-231 cells were transferred to 96-well plates (5000 cells per well) and allowed to attach and grow up to approximately 70% confluence. After incubation, the old media was removed, cells were washed and new media containing pure and functionalized SBA-15 silica materials with different composition (10, 25 and 50 μg mL^{-1}) in serum free DMEM media were added. After incubation for 72 h, 4-[3-(4-iodophenyl)-2-(4-nitrophenyl)-2*H*-5-tetrazolio]-1,3-benzene disulfonate (WST-1 reagent) was added to the cells and further incubated for 3 h; after which, the 96-well plate was analysed at a 430 nm wavelength in a Varioskan plate reader (Thermo Scientific, Logan UT) to determine cell viability. Here, the control group was the cell media only in the absence of particles.

2.5 Characterization techniques

X-ray powder diffraction (XRD) patterns were acquired on a PHILIPS X'PERT diffractometer using Cu Kα radiation. Data were recorded from 0.6 to 5º (2θ) with a resolution of 0.02º. N_2 adsorption–desorption isotherms at -196 ^{o}C were obtained in a Micromeritics Tristar 3000 system. Surface area was calculated by using the B.E.T. equation (P/P_o from 0.05 to 0.20) and the pore size distribution was obtained from the adsorption branch by means of the B.J.H. model assuming a cylindrical geometry of the pores. Degasification step prior to adsorption analyses was carried out under a nitrogen flux of 100 mL/min, at a temperature of 200 ^{o}C for pure silica SBA-15 and at 150 ^{o}C for organic-containing samples. Structural characterization was completed by transmission electron microscopy (TEM) in a PHILIPS TECNAI-10 electronic microscope operating at 200 kV.

Thermogravimetric analyses were performed under air atmosphere with a Star System Mettler Thermobalance in the temperature range from 40 to 700 ^{o}C at 5 ^{o}C·min^{-1}. The nitrogen content, corresponding to the amino groups incorporated with the functionalization agents, was measured by elemental analysis on a CHNOS model Vario EL III of Elemental Analyses System.

A Malvern ZetaSizer Nano-ZS from Malvern Instruments was used for obtaining the Zeta potential values of the particle suspensions. The samples were suspended in Phosphate Buffered Saline (PBS) with 1 mg·mL^{-1} concentration.

3. Results and discussion

3.1 Characterization of the synthesized hybrid materials

The low-angle X-ray diffraction patterns of the functionalized-SBA-15 samples synthesized by co-condensation or grafting methods are compiled in Figure 1 ((a) co-condensation, (b) grafting). For comparison purposes, the diffractions patterns of purely siliceous mesostructured SBA-15 are also included. In the case of materials synthesized using the co-condensation method, the organic template of the pure silica SBA-15 sample was removed by refluxing process (SBA-15-ext), while for materials synthesized using the grafting process, the surfactant

was removed by calcination (SBA-15-cal). XRD patterns show the presence of mesophases with hexagonal *p6mm* symmetry, since the characteristic 100, 110 and 200 diffractions are clearly distinguished in the samples prepared by both procedures [34]. Moreover, functionalized samples synthesized by grafting (Figure 1b) evidenced no alterations of the mesopore ordering as a result of the modification. Nevertheless, a slight reduction of intensity in the secondary reflections was observed for some modified samples as compared with the pure silica SBA-15-cal. This fact is normally caused by the partial pore filling with organic chains [5]. In the case of the functionalized-SBA-15 samples synthesized by co-condensation method (Figure 1a), the intensities of the secondary diffraction peaks are lower than those of SBA-15-ext silica material and samples synthesized by grafting technique. This reduction in the intensity is due to the typical structure-distorting phenomena observed when the ordered silica structure and the organic groups are incorporated in the same step [38]. Moreover, the intensity of the peaks gradually diminishes as the size of the incorporated organic chain is increased in samples prepared by both methods (Scheme 1 and Figure 1). However, even the samples synthesized by co-condensation procedure and with the longest chain displays a high ordering degree.

Figure 1

The TEM micrographs (Supporting Information Figure S1) confirm the ordered *p6mm* hexagonal structure of mesostructured SBA-15-type materials, independently of the synthesis route followed.

Nitrogen adsorption-desorption isotherms of all the samples synthesized (pure silica SBA-15-ext, pure silica SBA-15-cal and functionalized materials) are shown in Figure 2 ((a) co-condensation, (b) grafting). All the materials displayed typical type IV isotherms (IUPAC) with clear H1-type adsorption-desorption hysteresis loops, characteristic of SBA-15-type mesoporous materials [39]. For functionalized samples, the adsorbed nitrogen volume decreased and a slight deformation of the hysteresis loops was observed with respect to non-modified SBA-15 silicas, being especially remarkable in the case of the samples synthesized by co-

condensation method (Figure 2a). These results can be attributed to the framework perturbation that organosilane molecules introduce during the condensation process [40].

Figure 2

Textural properties (S_{BET}, V_{PORE}, D_{PORE}), wall thickness, efficiency in organic incorporation and Zeta potential values of pure and functionalized SBA-15 samples are summarized in Table 1. In addition, the pore size distribution of all the samples synthesized is also included in Figure S2. Mesoporous SBA-15 silica with the surfactant removed by calcination (SBA-15-cal) displays values of surface area, pore volume and pore diameter of 743 $m^2 \cdot g^{-1}$, 1.09 $cm^3 \cdot g^{-1}$ and 8.3 nm, respectively, while in the case of the SBA-15 with the organic template extracted with ethanol (SBA-15-ext) the values are 689 $m^2 \cdot g^{-1}$, 0.99 $cm^3 \cdot g^{-1}$ and 8.2 nm, respectively. This slight shrinking of pore volume and surface area observed for SBA-15-ext material is due to less efficient elimination of the surfactant from the meso- and micropores than in the SBA-15-cal sample, in which the template is calcined. Functionalized samples exhibit a lower surface area and pore volume values than those of pure silica SBA-15 silica materials, as expected, due to the incorporation of the organic molecules onto the mesostructured silica support. However, this decline in the textural properties depends on the synthesis procedure. Thus, in the case of the materials functionalized by grafting, a remarkable reduction in the BET surface area is observed with respect to the same sample synthesized by co-condensation, which is attributed to the different location of the incorporated organosilane moieties. In the grafting approach, the organosilane moieties are covalently attached to the surface silanol species of the mesoporous SBA-15 silica material, filling partially the pores with the organic molecules, and therefore reducing in part the porosity of the sample. However, for the silica materials synthesized by direct synthesis, the organic groups are incorporated during the condensation process into the pore-wall network, modifying in a lower degree the porosity of the material. Thus, the surface-functionalized silica materials synthesized using co-condensation method show higher wall thickness values than the same silica material synthesized by grafting technique. Since co-condensation of trialkoxyorganosilanes with tetraalkoxysilanes in the presence of structure-directing agents takes place, the increase in the wall thickness is attributed to the fraction of the

organic groups located into the pore-wall network. The organic incorporation, respect to the theoretical maximum value, is remarkably high in all the cases, especially for samples functionalized by co-condensation. Furthermore, Zeta potential measurements were carried out to characterize the net surface charge of the samples at neutral pH. The Zeta potential value of the pure silica SBA-15-cal sample is -18.6 mV while the value of pure silica SBA-15-ext is -21.4 mV. This parameter is associated to the free silanol groups on the surface of the SBA-15 materials, higher in the sample where the surfactant template was removed by extraction (SBA-15-ext). However, for the functionalized samples, the obtained Zeta potential comprise a range of values, from highly negatives to positives. The latter are obtained for materials incorporating aminopropyl groups (AP-SBA-15-C and AP-SBA-15-G), what indicates the successful incorporation of the functionality onto the surface of the silica supports [41].

Table 1

3.2 Drug loading and release for functionalized samples synthesized by co-condensation and grafting.

Several experiments have been conducted in order to modify the surface of mesoporous SBA-15 silica materials by incorporating different organosilane groups by co-condensation and grafting. Methylprednisolone sodium hemisuccinate was chosen as model drug, and its loading and release from the functionalized SBA-15 silica particles were *in vitro* evaluated. Figure 3a shows the amount of guest drug loaded and released in 4 days from the pure silica SBA-15-cal, SBA-15-ext samples and functionalized SBA-15 materials. The drug loading degree resulted independent of the organosilane incorporation method onto the silica-surface. However, the organosilane type was proved to exert a clear influence on the guest drug adsorption on the modified silica surface [42, 43]. The adsorption of the drug is basically a surface phenomenon and it must be a function of the chemical affinity between the surface and the drug. From previous studies of our group [37], it was established that the differences in drug loadings among these type of silica materials can be explained by the hydrogen-bonding and electrostatic interactions among the guest drugs and silica surfaces. Drug adsorption process may occur via

hydrogen-bonding of carboxylate moieties to surface silanol sites as well as by intermolecular interactions among the functionalized alkyl chains and methylprednisolone moieties. Thus, as the Zeta potential of pure methylprednisolone sodium hemisuccinate is -23.0 mV (measured at pH 7.4), these species will have stronger attractive electrostatic interactions with, and greater adsorption to, silica surfaces having greater positive charge. SBA-15 functionalized with aminopropyl groups (AP-SBA-15-C and AP-SBA-15-G) are the unique samples which have a positive Zeta potential values (13.6 and 5.9 mV respectively, Table 1) and the results showed that its methylprednisolone adsorption capacity was the greatest, while pristine and modified mesoporous materials with negative Zeta potential values exhibited remarkably lower drug loading capacities.

Drug-release values after 4 days for the different mesoporous SBA-15 silica materials are also displayed in Figure 3a. All *in vitro* studies have been performed under a pH of 7.4 in the same conditions (see experimental section). The results show that those materials with higher drug loading correlates well with a higher amount of drug released. Moreover, the samples synthesized by co-condensation method display a different behaviour that the materials synthesized by grafting technique. Samples synthesized by co-condensation show faster drug delivery than the same samples synthesized by grafting technique, which slows down the drug release, and hence driving a more controlled *in vitro* drug administration, as shown in Figure S3. This result can be explained on the basis of the functionality location on the silica-surface, much more accessible for grafting incorporation strategies that enable stronger interactions between methylprednisolone molecules and the organosilane moieties anchored onto the mesoporous SBA-15 silica materials. The silica materials with aminopropyl organosilane functionalities have been shown to be particularly effective in the drug controlled administration, since the final positively charged aminopropyl groups can strongly interact with the negatively charged methylprednisolone, as deduced from the Zeta potential measurements, retarding the drug delivery. Such as Figure 3b shows, for each drug concentration, the release rate of AP-SBA-15-G sample was slower than AP-SBA-15-C sample. The same tendency is observed for the rest of the materials, as displayed in Figure S4. The better dosage of the drug

concentration for the sample synthesized by grafting route is very recommend in well water-soluble drugs, as for instance methylprednisolone sodium hemisuccinate, to impede a burst drug release before reaching the objectives on body. As conclusion, functionalized SBA-15 mesoporous silicas have been proved to be successful in establishing strong interactions among the drug and organosilane moieties that decorates the silica surface. These nanosilicas drug delivery vehicles would allow to reach out the damaged organs on body with enough cargo to be effective. There are multiple applications where is necessary providing a sustained release of this type of drug (corticoids) over long period of time [44].

Figure 3

3.3 Drug loading and release over different amino organosilanes-modified SBA-15 materials synthesized by grafting.

According to the results above commented in section 3.2, the silica materials functionalized with molecules containing amino groups have shown to be particularly effective in the drug controlled administration. For this reason, the second objective of this research work was to explore different amino organosilane moieties to modify the SBA-15 silica surface via grafting procedure, to improve the loading and the controlled drug delivery. To evaluate the influence of the amino-organosilane structure, several precursors (Scheme 1) have been incorporated by grafting in SBA-15 materials: 3-(aminopropyl)trimethoxysilane (AP), *N*-(3-trimethoxysilylpropyl) ethylenediamine (ED), *N*-(3-trimethoxysilylpropyl)diethylenetriamine (DT), (*N*-phenylaminopropyl) trimethoxysilane (PAP) and (aminoethylaminomethyl) phenethyltrimethoxysilane (AEMP3).

XRD patterns of the modified SBA-15 materials (Figure S5a) showed the characteristic reflections of SBA-15 pure silica materials, (1 0 0), (1 1 0) and (2 0 0), verifying the hexagonal

order maintenance. All the materials displayed typical type IV isotherms (IUPAC) with clear H1-type adsorption-desorption hysteresis loops, characteristic of mesoporous SBA-15-type materials (Figure S5b). Pore size, BET surface area and pore volume values of the reference SBA-15-cal and the surface amino-modified SBA-15 materials are summarized in Table 2. Analyses of N_2 adsorption data reveal a significantly reduced BET surfaces areas for functionalized SBA-15 materials (332-441 m^2g^{-1} sample) with respect to SBA-15-cal silica (743 m^2g^{-1} sample), which results from the added mass associated with grafted amino-organosilica species. Although the pore volumes of amino-modified SBA-15 materials (0.62-0.73 cm^3g^{-1} silica) are quite lower than the corresponding to SBA-15-cal silica (1.09 cm^3g^{-1} silica), successful amino-organosilane incorporations have been achieved. Specifically, for AEMP3-SBA-15-G sample modified with the longest and bulkiest organosilane, it is noticeable the reduction in the pore volume of 50 % with respect to the SBA-15 pure silica sample (Table 2).

The quantities of amino-organosilanes species grafted to the surface of SBA-15 pure silica are obtained from thermogravimetric analysis and are summarized in Table 2. The nitrogen content of the modified SBA-15 materials was measured by elemental analysis, and can be directly related to the amounts of grafted amino-organosilica species and with the number of nitrogen atoms contained in the amino-organosilane employed for the functionalization. Thus, DT-SBA-15-G material showed the maximum nitrogen content (3.21 $mmolN \cdot g^{-1}_{MAT}$).

Table 2

The drug adsorption capacities of SBA-15-cal and amino-modified SBA-15 are determined and shown in Table 2 to correlate qualitatively with the strengths of electrostatic interactions between methylprednisolone and the organo-silica surfaces, along with the textural properties of the samples. Subsequent UV-Vis analyses establish methylprednisolone loadings of 109 $mg_{DRUG}.g^{-1}_{MAT}$ of SBA-15-cal for pure silica SBA-15-cal, and remarkable greater loadings for amino-modified materials, up to 467 $mg_{DRUG}.g^{-1}_{MAT}$ for sample DT-SBA-15-G. Differences in methylprednisolone loadings among these organo-materials can be explained by the electrostatic

interactions among the drug and organo-silica surfaces, correlated with the nitrogen loading of each sample. Thus, DT-SBA-15-G material has four time drug loading (467 $mg_{DRUG}.g^{-1}_{MAT}$) with respect to SBA-15-cal sample, which is also the sample with higher nitrogen content. It is interesting to notice that the adsorbed methylprednisolone amount was only 150 $mg_{DRUG}.g^{-1}_{MAT}$ for the material modified with (*N*-phenylaminopropyl)trimethoxysilane (PAP-SBA-15-G), the one with the lower nitrogen content and more negative Zeta potential value due to the charge delocalization with the aromatic group [45].

DT-SBA-15-G material has the most positive Zeta potential among the alkyl amino-modified materials (12.3 mV at pH 7.4, Table 2) and the greatest methylprednisolone loading capacity, while mesoporous SBA-15-cal pure silica, with the most negative Zeta potential (-18.6 mV at pH 7.4), exhibits the lowest loading capacity, which demonstrates the importance of attractive electrostatic interactions for the drug adsorption process. Regarding the aromatic amino-modified materials, AEMP3-SBA-15-G sample presents the most positive Zeta potential among the materials tested (16.4 mV at pH 7.4) and a remarkable, but not the largest drug loading capacity (330 $mg_{DRUG}.g^{-1}_{MAT}$). This result demonstrates that attractive electrostatic interactions are not solely the responsible for methylprednisolone loading, but the nitrogen content. Comparing DT-SBA-15-G and AEMP3-SBA-15-G materials, it is manifested that both samples possess similar textural properties, and the aminophenyl exhibits even higher Zeta potential than aminoalkyl organosilane, which would drive to obtain higher loading of methylprednisolone. However, the results indicate the opposite, and the likely explanation resides in the lower N content of the aromatic AEMP3-SBA-15-G sample, which clearly conducts to lower drug loading. In addition, to support this conclusion, we found the same fact when AP-SBA-15-G and ED-SBA-15-G are compared. Both materials show similar textural properties and Zeta potential, but higher nitrogen amount in the case of ED-SBA-15-G material, which conducts to obtain a significant higher drug loading (see Table 2).

The amounts of methylprednisolone species released from organo-modified mesoporous silica materials into simulated body fluids under near neutral conditions (pH 7.4), corresponding to

those in the blood stream, can be estimated by using UV-visible spectroscopy (absorbance at 247 nm). In Figure 4a, the methylprednisolone delivery concentration from organo-modified materials is displayed. Delivery data of pure silica SBA-15-cal have been included for comparative purposes. Normalizing the amounts of released methylprednisolone species to the initial mass of methylprednisolone contained in the organo-modified mesoporous silica materials, yield the percentage of methylprednisolone released from these materials, as depicted in Figure 4b.

The release of methylprednisolone was gradual and sustained over time for every functionalized sample compared to the typical burst release that occurs when the drug is located at the outer external surface of the porous siliceous materials. Depending on the molecular group containing the nitrogen atoms for the different samples, the release time is extended from two to ten days. Thus, the more nitrogen atoms comprising the aliphatic chain hydrocarbon moiety, the slower the methylprednisolone release. Same trend is observable for both aromatic amino-organosilanes employed for the functionalization, AEMP3 and PAP materials.

In order to understand the kinetic model and mechanism that describe the overall drug release, the results of the *in vitro* methylprednisolone release were fitted to a well-known drug release kinetic equation, the Korsmeyer-Peppas [46] model. From the calculated R^2 values, listed in Supporting Information Table S1, it is apparent that the experimental data on drug release fit well to Korsmeyer-Peppas model. The “n” exponent may be used to characterize the release mechanism. Thus, the n values were higher than 0.5 (Table S1) for all the materials except for the SBA-15-cal sample. These values are characteristic for mass transfer following a non-Fickian model, suggesting that the diffusion of methylprednisolone from amino modified mesoporous materials is impeded or restricted by the interactions among the drug and the amino groups anchored to the surface silica species. Additionally, the methylprednisolone released from the modified silica hosts were fitted a first-order kinetic. The release rates of methylprednisolone from amino-modified silica hosts were calculated by the derivative of the given cumulative release profile at a specific point in time and are displayed in Figure S6. The first-order rate coefficients were also calculated from the release rate plot at low drug release

concentration (Table S1) when the kinetic model is first-order with respect to the drug release amount. Analyses of the cumulative methylprednisolone release profiles using the first-order kinetic model reveal that the lowest first-order rate coefficient is associated with the DT materials (0.71 min^{-1}, Table S1), which is the material with the larger amount of nitrogen atom in its structure, compared to PAP or AP materials (2.33 and 3.95 min^{-1}, respectively) with the less amount of nitrogen atoms in their framework. Although the use of more complex mathematical modelling would result very useful to the more accurately predict the kinetic release values, and some others physical parameters such as the diffusion coefficients [47, 48], the Korsmeyer-Peppas equation provided enough information about the drug transport mechanism, and which is better, the comparison of the raw and functionalized mesoporous silica materials in the same conditions.

Figure 4

Exposure of N-functionalized mesoporous silica materials to simulated body fluids under acidic conditions, pH 4.6 (Figure 5), corresponding to those nearby the stomach or tumors, yields similar percentages of drug release and slower kinetics than those obtained at near neutral conditions, pH 7.4. The lower rates of methylprednisolone released at this low pH (Figure S6) are consistent with the increased attractive electrostatic interactions among methylprednisolone and the functionalized silica surfaces under acidic versus near neutral conditions, as evidenced by the Zeta potential measurements (Table 2) of the corresponding materials. Analyses of methylprednisolone release profiles into acidic simulated body (Table S1) using the Korsmeyer-Peppas model reveal similar non-Fickian diffusion processes for methylprednisolone in every N-functionalized material, as observed under near neutral conditions.

Figure 5

Finally, the *in vitro* cytocompatibility of the more significant hybrid materials prepared was examined on cultured MDA-MB-231 Breast cancer cells adopting the WST-1 assay [49]. The cells were exposed for 72 h to the medium containing the selected mesoporous materials (SBA-15 calc, AP-SBA-15-G, AP-SBA-15-C and DT-SBA-15-G) in the concentration range of 10-50

μg mL^{-1} (Figure 6). WST-1 assay results revealed that the mesoporous materials were not cytotoxic towards the cells (> 80% viability), although a slight decrease in cell proliferation was observed as compared to the untreated cells. These results are in agreement with previous studies [50, 51], indicating that silica-based mesoporous materials induce no cytotoxic effects on the cells.

Figure 6

4. Conclusions.

Mesoporous SBA-15 materials functionalized with several functionalities and prepared using both, the direct synthesis (co-condensation) and the post-synthesis grafting methods, have been evaluated for their ability to load and release the glucocorticoid methylprednisolone sodium hemisuccinate model drug. These hybrid silica carriers have displayed a good mesoscopic ordering and textural properties, in combination with a high organic incorporation yield respect to the theoretical value. The adsorption capacity and release behavior of drug in these modified silica matrix were dependent on the type of functionality incorporated and the synthesis route followed. Specifically, the functionalization with organosilanes containing an amino group, in particular aminopropyl, were the materials with the highest drug loading capacities. This result was attributed to the strong electrostatic interactions between the hydrophilic model drug and the polar amino moieties also with hydrophilic character. It was unclear the dependency of drug loading degree related to the route synthesis followed. However, overall, the samples synthesized by co-condensation method exhibited higher uncontrolled drug delivery than the materials synthesized by grafting technique. This different behaviour was attributed to location of the functionality, more accessible in the case of the grafting process, and hence with higher interactions between the functionalities and corticoid. Afterwards, in order to improve the corticoid loading and establish a better control of drug delivery, different amino-organosilanes were incorporated into SBA-15 material via grafting procedure. The higher number of amino groups incorporate into SBA-15 material, the greatest drug loading capacity, and the better control in the drug delivery. The DT-SBA-15-G material with 3.21 mmol $N.g^{-1}$ is the material

that incorporated the greatest amount of drug (467 $mg_{DRUG}.g^{-1}_{MAT}$), and exhibiting the more gradual and sustained drug release over time. Moreover, a decrease in the pH of the release media from 7.4 to 4.6 (typical in zones close to tumours) produces a reduction in the kinetics of methylprednisolone release due to increased attractive electrostatic interactions among drug and the functionalized silica surfaces under acidic versus near neutral conditions. Non-Fickian diffusion processes for methylprednisolone release in every N-functionalized material were observed under either near neutral or acidic conditions. Finally, it was confirmed that the synthesized silica mesoporous materials induce no cytotoxic effects on the cells in a silica concentration range of 10-50 $\mu g \cdot mL^{-1}$.

Acknowledgements.

The financial support of the Spanish government (CTQ2011-22707, CTQ2014-57858-R) is gratefully acknowledged.

References.

[1] L. Cao, T. Man, M. Kruk, Chem. Mater. 21 (2009) 1144-1153.

[2] M. Moritz, M. Geszke-Moritz, Mater. Sci. Eng. C 49 (2015) 114-151.

[3] J.M. Rosenholm, C. Sahlgren, M. Lindén, Nanoscale 2 (2010) 1870-1883.

[4] M. Manzano, M. Vallet-Regi, J. Mater. Chem. 20 (2010) 5593-5604.

[5] V. Morales, M.N. Idso, M. Balabasquer, B. Chmelka, R.A. García-Muñoz, J. Phys. Chem. C 120 (2016) 16887-16898.

[6] E. Ghedini, M. Signoretto, F. Pinna, V. Crocellà, L. Bertinetti, G. Cerrato, Microporous Mesoporous Mater. 132 (2010) 258-267.

[7] M. Vallet-Regí, J.C. Doadrio, A.L. Doadrio, I. Izquierdo-Barba, J. Pérez-Pariente, Solid State Ionics 172 (2004) 435-439.

[8] R. Mellaerts, R. Mols, J.A. Jammaer, C.A. Aerts, P. Annaert, J. Van Humbeeck, G. Van den Mooter, P. Augustijns, J.A. Martens, Eur. J. Pharm. Biopharm. 69 (2008) 223-230.

[9] S.-Y. Park, M. Barton, P. Pendleton, Colloids Surf. A 385 (2011) 256-261.

[10] A.L. Doadrio, E.M.B. Sousa, J.C. Doadrio, J. Pérez Pariente, I. Izquierdo-Barba, M. Vallet-Regí, J. Control. Release 97 (2004) 125-132.

[11] F. Sevimli, A. Yilmaz, Microporous Mesoporous Mater. 158 (2012) 281-291.

[12] J.A. Melero, G.D. Stucky, R. van Grieken, G. Morales, J. Mater. Chem. 12 (2002) 1664-1670.

[13] A. Martin, G. Morales, F. Martinez, R. van Grieken, L. Cao, M. Kruk, J. Mater. Chem. 20 (2010) 8026-8035.

[14] X.Y. Liu, L. Zhu, T. Zhao, J.F. Lan, W.F. Yan, H.X. Zhang, Microporous Mesoporous Mater. 142 (2011) 614-620.

[15] A. Szegedi, M. Popova, I. Goshev, J. Mihály, J. Solid State Chem. 184 (2011) 1201-1207.

[16] A. Martín, R.A. García, D.S. Karaman, J.M. Rosenholm, J. Mater. Sci. 49 (2014) 1437-1447.

[17] Q. Tang, Y. Chen, J. Chen, J. Li, Y. Xu, D. Wu, Y. Sun, J. Solid State Chem. 183 (2010) 76-83.

[18] B.-S. Tian, C. Yang, J. Phys. Chem. C 113 (2009) 4925-4931.

[19] C. Gu, P.A. Chia, X.S. Zhao, Appl. Surf. Sci. 237 (2004) 387-392.

[20] J. Yang, J. Zhang, L. Zhu, S. Chen, Y. Zhang, Y. Tang, Y. Zhu, Y. Li, J. Hazard. Mater. 137 (2006) 952-958.

[21] V. Morales, M. Gutiérrez-Salmerón, M. Balabasquer, J. Ortiz-Bustos, A. Chocarro-Calvo, C. García-Jiménez, R.A. García-Muñoz, Adv. Funct. Mater. (2016) DOI:10.1002/adfm.201505073.

[22] R.A. Garcia, V. Morales, T. Garces, J. Mater. Chem. 22 (2012) 2607-2615.

[23] R. van Grieken, J. Iglesias, V. Morales, R.A. García, Microporous Mesoporous Mater. 131 (2010) 321-330.

[24] R.A. García-Muñoz, V. Morales, M. Linares, B. Rico-Oller, Langmuir 30 (2014) 881-890.

[25] A.S. Maria Chong, X.S. Zhao, A.T. Kustedjo, S.Z. Qiao, Microporous Mesoporous Mater. 72 (2004) 33-42.

[26] F. Bernardoni, A.Y. Fadeev, J. Colloid Interf. Sci. 356 (2011) 690-698.

[27] A. Stein, B.J. Melde, R.C. Schroden, Adv. Mater. 12 (2000) 1403-1419.

[28] M.H. Lim, A. Stein, Chem. Mater. 11 (1999) 3285-3295.

[29] C. Lesaint, B. Lebeau, C. Marichal, J. Patarin, Microporous Mesoporous Mater. 83 (2005) 76-84.

[30] N. García, E. Benito, J. Guzmán, P. Tiemblo, V. Morales, R.A. García, Microporous Mesoporous Mater. 106 (2007) 129-139.

[31] A.C.P. Sagcal-Gironella, C.M.T. Sherwin, R.G. Tirona, M.J. Rieder, H.I. Brunner, A.A. Vinks, Clin. Therapeutics 33 1524-1536.

[32] A.A. Bhirde, V. Patel, J. Gavard, G. Zhang, A.A. Sousa, A. Masedunskas, R.D. Leapman, R. Weigert, J.S. Gutkind, J.F. Rusling, ACS Nano 3 (2009) 307-316.

[33] J.M. Rosenholm, C. Sahlgren, M. Linden, Curr. drug targets 12 (2011) 1166-1186.

[34] D. Zhao, J. Feng, Q. Huo, N. Melosh, G.H. Fredrickson, B.F. Chmelka, G.D. Stucky, Science 279 (1998) 548-552.

[35] D. Kumar, K. Schumacher, C. du Fresne von Hohenesche, M. Grün, K.K. Unger, Colloids Surf. A 187–188 (2001) 109-116.

[36] J.M. Rosenholm, M. Lindén, Chem. Mater. 19 (2007) 5023-5034.

[37] R.A. Garcia-Munoz, V. Morales, M. Linares, P.E. Gonzalez, R. Sanz, D.P. Serrano, J. Mater. Chem. B 2 (2014) 7996-8004.

[38] G. Morales, R. van Grieken, A. Martín, F. Martínez, Chem. Eng. J. 161 (2010) 388-396.

[39] F. Rouquerol, J. Rouquerol, K. Sing, Academic Press, London, 1999.

[40] X. Wang, K.S.K. Lin, J.C.C. Chan, S. Cheng, J. Phys. Chem. B 109 (2005) 1763-1769.

[41] J. Pang, L. Zhao, L. Zhang, Z. Li, Y. Luan, J. Colloid Interface Sci. 395 (2013) 31-39.

[42] S.W. Song, K. Hidajat, S. Kawi, Langmuir 21 (2005) 9568-9575.

[43] F. Qu, G. Zhu, S. Huang, S. Li, S. Qiu, Chemphyschem 7 (2006) 400-406.

[44] M. Fernandez, J. Parra, B. Vazquez, A. Lopez-Bravo, J.S. Román, Biomaterials 26 (2005) 3311-3318.

[45] M.E. Vaschetto, B.A. Retamal, J. Phys. Chem. A 101 (1997) 6945-6950.

[46] R.W. Korsmeyer, R. Gurny, E. Doelker, P. Buri, N.A. Peppas, J. Pharm. Sci. 15 (1983) 25-35.

[47] I. Galdi, G. Lamberti, Heat Mass Transfer 48 (2012) 519-528.

[48] M. Manzano, G. Lamberti, I. Galdi, M. Vallet-Regí, AAPS PharmSciTech 12 (2011) 1193-1199.

[49] M. Ishiyama, H. Tominaga, M. Shiga, K. Sasamoto, Y. Ohkura, K. Ueno, Biol. Pharm. Bull. 19 (1996) 1518-1520.

[50] J. Zhang, D. Desai, J.M. Rosenholm, Adv. Funct. Mater. 24 (2014) 2352-2360.

[51] D. Desai, S. Karaman, N. Prabhakar, S. Tadayon, A. Duchanoy, M. Toivola, S. Rajput, T. Näreoja, J. Rosenholm, Mesoporous Biomater. 1 (2014) 16-43.

Table list

Table 1. Textural properties, organosilane yield and Zeta potential values of the synthesized materials.

Material	S_{BET} ($m^2.g^{-1}$)	V_p [a] ($cm^3.g^{-1}$)	D_p [a] (nm)	Wall Thickness[b] (nm)	Organosilane Incorporation[c] (%)	Zeta Potential[d] (mV)
SBA-15-ext	689	0.99	8.2	3.0	-	-21.4
SBA-15-cal	743	1.09	8.3	3.1	-	-18.6
AP-SBA-15-C	560	0.74	8.1	4.8	92.3	13.6
AP-SBA-15-G	420	0.70	7.9	3.5	84.6	5.9
AS-SBA-15-C	648	0.83	8.2	5.3	85.1	-27.0
AS-SBA-15-G	394	0.74	7.6	3.4	73.2	-26.8
MP-SBA-15-C	681	0.90	8.0	3.6	89.2	-14.3
MP-SBA-15-G	421	0.87	7.9	3.5	82.1	-14.6
TM-SBA-15-C	591	0.89	8.1	3.9	92.3	-14.1
TM-SBA-15-G	448	0.89	8.0	3.1	90.2	-11.9
SE-SBA-15-C	573	0.72	7.3	4.9	85.0	-12.3
SE-SBA-15-G	435	0.70	7.1	4.8	72.1	-9.90
OC-SBA15-C	627	0.94	8.2	3.3	78.8	-12.1
OC-SBA15-G	455	0.83	8.0	3.2	63.2	-3.80
NF-SBA-15-C	653	0.93	8.2	3.4	80.1	-14.0
NF-SBA-15-G	584	0.88	8.1	3.3	71.8	-10.0
Methylprednisolone						-23.0

[a] Total pore volume and pore size as calculated by the BJH method from the adsorption branch of the N2 isotherm [b] Pore wall thickness calculated as the difference between the lattice parameter (a_0) and the mean pore diameter (Dp), being $a_0=2d(100)/\sqrt{3}$ [c] Organic content determined via weight loss by TGA in the range 110-700 ^{0}C [d] at neutral pH

Table 2. Textural and organic properties of the amino-modified materials.

Material	S_{BET} ($m^2.g^{-1}$)	V_p [a] ($cm^3.g^{-1}$)	D_p [a] (nm)	e [b] (nm)	Z-Potential (mV)		N Content [c] ($mmolN.g^{-1}_{MAT}$)	Organosilane Incorporation [d] (%)	Adsorbed drug ($mg_{DRUG}.g^{-1}_{MAT}$)
					pH 7.4	pH 4.6			
SBA-15-cal	743	1.09	8.3	3.1	-18.6	-4.9	-	-	109
AP-SBA-15-G	420	0.70	7.9	3.5	5.9	24.1	1.57	84.6	242
ED-SBA-15-G	433	0.68	7.1	3.8	7.2	25.5	2.50	91.8	372
DT-SBA-15-G	371	0.62	7.0	3.3	12.3	26.4	3.21	97.8	467
PAP-SBA-15-G	441	0.73	6.7	4.0	-11.1	8.0	1.16	88.6	150
AEMP3-SBA-15-G	332	0.56	6.8	4.5	16.4	30.1	2.21	95.4	330
Methylprednisolone					-23.0	-19.4			

[a] Total pore volume and pore size as calculated by the BJH method from the adsorption branch of the N2 isotherm [b] Pore wall thickness calculated as the difference between the lattice parameter (a_0) and the mean pore diameter (Dp), being $a_0=2d(100)/\sqrt{3}$.[c] Nitrogen content determined via elemental analysis. [d] Organic content determined via weight loss by TGA in the range 110-700 ^{0}C

Figure captions

Scheme 1. Selected organosilanes anchored by co-condensation and/or grafting on the SBA-15; i) 3-(aminopropyl)trimethoxysilane (AP), ii) 2-(4chlorosulfonylphenyl)ethyltrimethoxysilane (AS), iii) 3-(mercaptopropyl)trimethoxysilane (MP), iv) chlorotrimethylsilane (TM), v) styrylethyltrimethoxysilane (SE), vi) trimethoxy(octyl)silane (OC), vii) 1-naphthyltrimethoxysilane (NF), viii) *N*-(3-trimethoxysilylpropyl)ethylenediamine (ED), ix) *N*-(3-trimethoxysilylpropyl)diethylenetriamine (DT), x) (*N*-phenylaminopropyl)trimethoxysilane (PAP) and xi) (aminoethylaminomethyl) phenethyltrimethoxysilane (AEMP3). Organosilane size measured by ACD/ChemSketch 12.0 Software.

Figure 1. X-ray diffraction patterns for pure silica SBA-15 extracted and calcined, and functionalized SBA-15 materials synthesized by (a) co-condensation (b) grafting.

Figure 2. Nitrogen adsorption isotherms at 77 K for pure silica SBA-15-cal, SBA-15-ext material and functionalized samples synthesized by (a) co-condensation (b) grafting.

Figure 3. (a) Amount of methylprednisolone hemisuccinate adsorbed and released in 4 days by the pure and modified mesoporous SBA-15 silica materials; (b) Release rate of methylprednisolone from AP-SBA-15-C and AP-SBA-15-G materials into simulated body fluid at pH 7.4.

Figure 4. (a) Drug delivery in terms of concentration and (b) fractions of methylprednisolone released from the silica SBA-15 sample and functionalized SBA-15 materials at pH 7.4.

Figure 5. (a) Drug delivery in terms of concentration and (b) fractions of methylprednisolone released from the silica SBA-15 sample and functionalized SBA-15 materials at pH 4.6.

Figure 6. In vitro dose dependent cytocompatibility of SBA-15 and amino-functionalized SBA-15 materials after 72 h of incubation time on MDA-MB-231 Breast cancer cell lines. Cell viability was measured by the WST-1 assay. Error bars represent SD ($n \geq 3$).

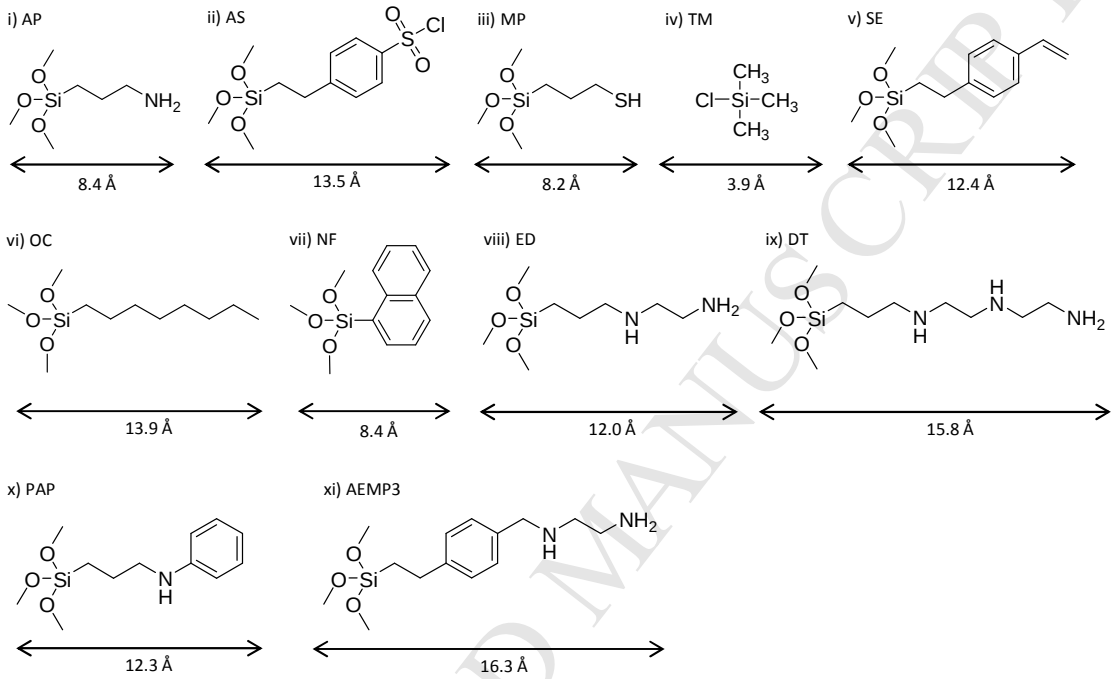

Scheme 1. Selected organosilanes anchored by co-condensation and/or grafting on the SBA-15; i) 3-(aminopropyl)trimethoxysilane (AP), ii) 2-(4chlorosulfonylphenyl)ethyltrimethoxysilane (AS), iii) 3-(mercaptopropyl)trimethoxysilane (MP), iv) chlorotrimethylsilane (TM), v) styrylethyltrimethoxysilane (SE), vi) trimethoxy(octyl)silane (OC), vii) 1-naphthyltrimethoxysilane (NF), viii) *N*-(3-trimethoxysilylpropyl)ethylenediamine (ED), ix) *N*-(3-trimethoxysilylpropyl)diethylenetriamine (DT), x) (*N*-phenylaminopropyl)trimethoxysilane (PAP) and xi) (aminoethylaminomethyl) phenethyltrimethoxysilane (AEMP3). Organosilane size measured by ACD/ChemSketch 12.0 Software.

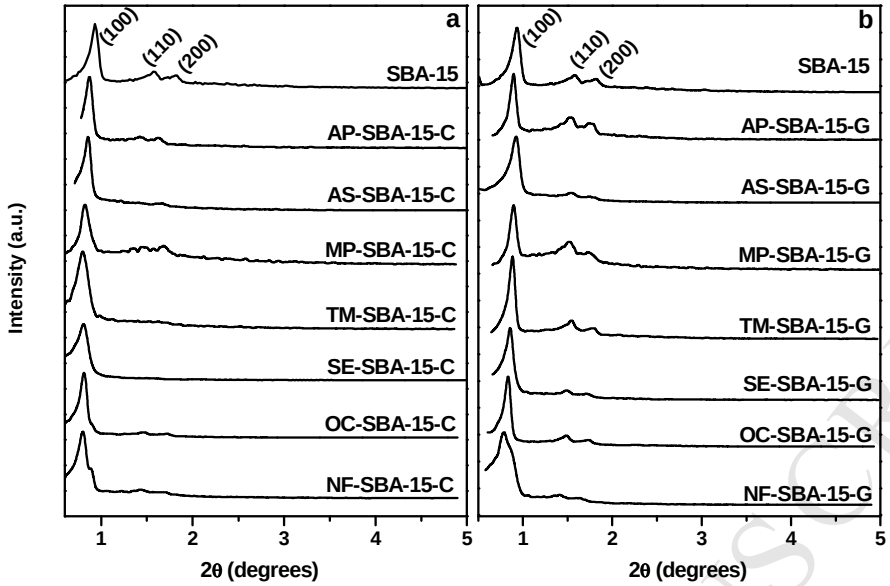

Figure 1. X-ray diffraction patterns for pure silica SBA-15 extracted and calcined, and functionalized SBA-15 materials synthesized by (a) co-condensation (b) grafting.

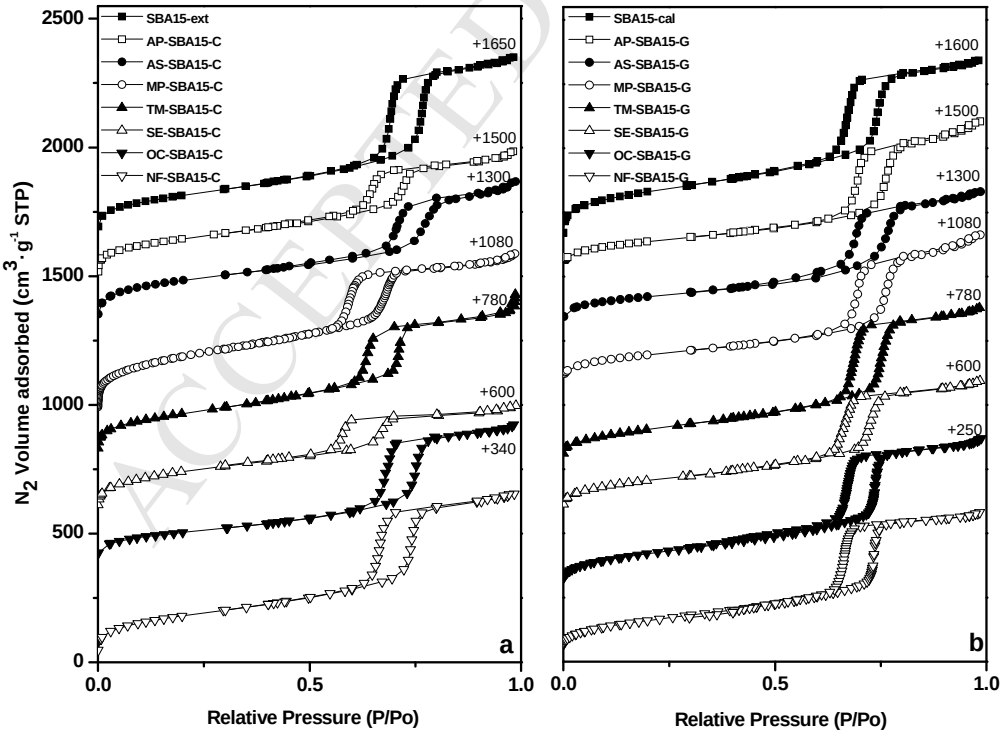

Figure 2. Nitrogen adsorption isotherms at 77 K for pure silica SBA-15-cal, SBA-15-ext material and functionalized samples synthesized by (a) co-condensation (b) grafting.

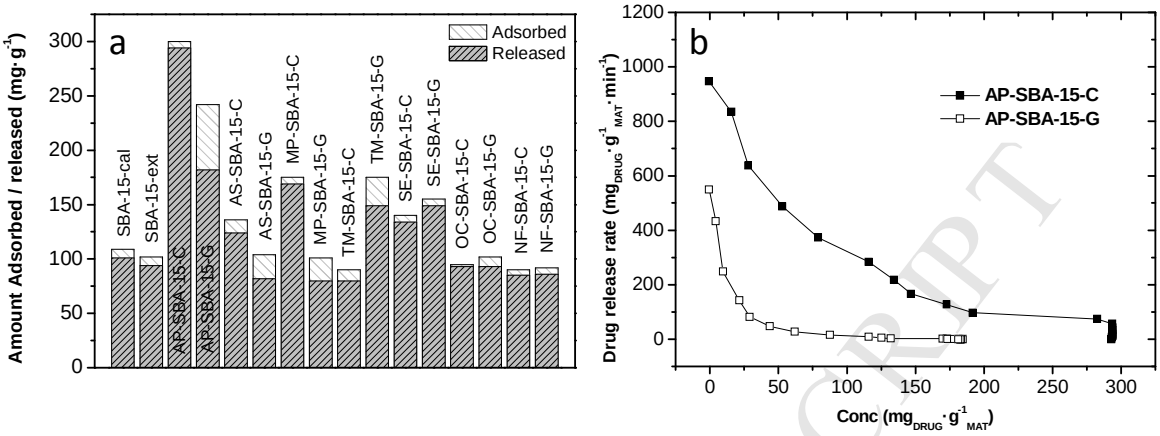

Figure 3. (a) Amount of methylprednisolone hemisuccinate adsorbed and released in 4 days by the pure and modified mesoporous SBA-15 silica materials; (b) Release rate of methylprednisolone from AP-SBA-15-C and AP-SBA-15-G materials into simulated body fluid at pH 7.4.

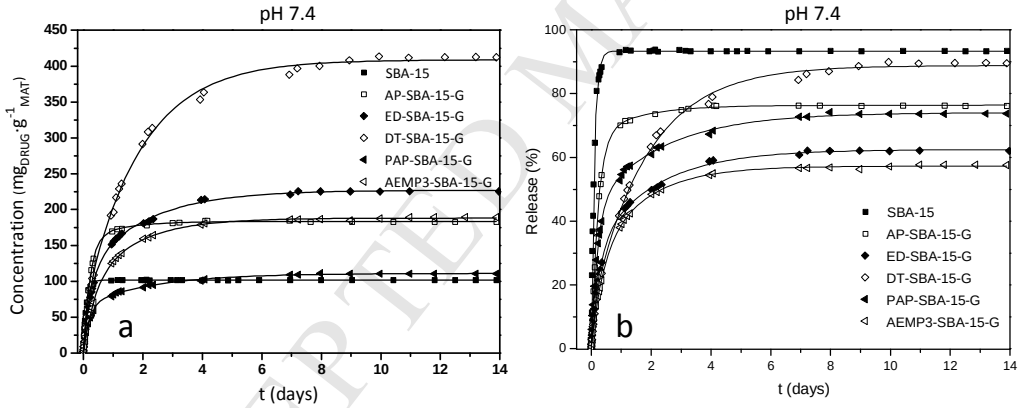

Figure 4. (a) Drug delivery in terms of concentration and (b) fractions of methylprednisolone released from the silica SBA-15 sample and functionalized SBA-15 materials at pH 7.4.

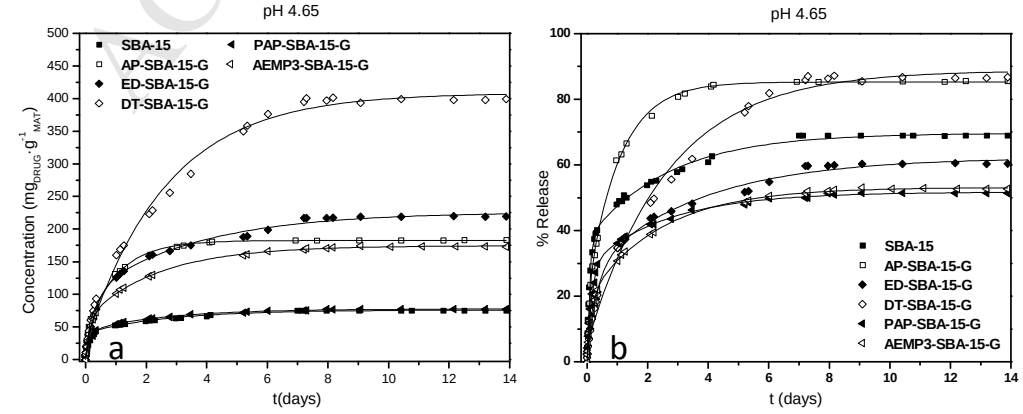

Figure 5. (a) Drug delivery in terms of concentration and (b) fractions of methylprednisolone released from the silica SBA-15 sample and functionalized SBA-15 materials at pH 4.6.

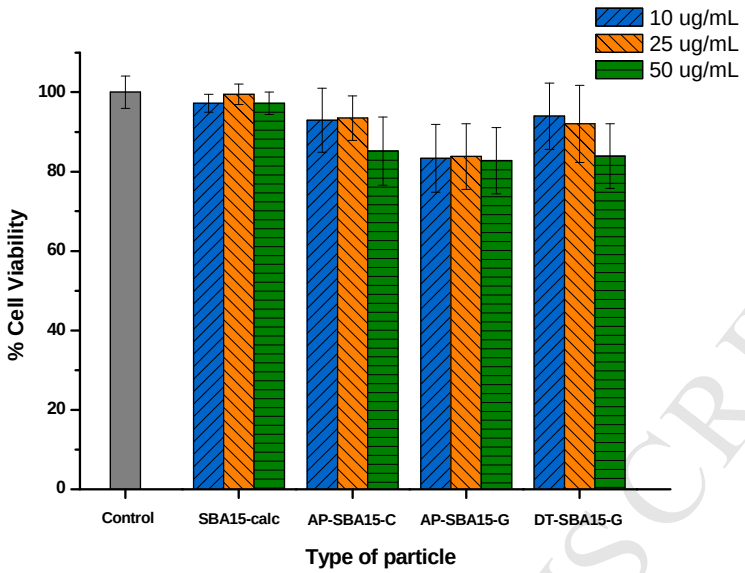

Figure 6. *In vitro* dose dependent cytocompatibility of SBA-15 and amino-functionalized SBA-15 materials after 72 h of incubation time on MDA-MB-231 Breast cancer cell lines. Cell viability was measured by the WST-1 assay. Error bars represent SD ($n \geq 3$)

Supporting Information

Surface-functionalization of mesoporous SBA-15 silica materials for controlled release of methylprednisolone sodium hemisuccinate: influence of functionality type and strategies of incorporation

J. Ortiz-Bustos, A. Martín, V. Morales, R. Sanz, and R. A. García-Muñoz

Chemical and Environmental Engineering Group, Universidad Rey Juan Carlos, C/ Tulipán s/n, 28933 Móstoles, Madrid, Spain

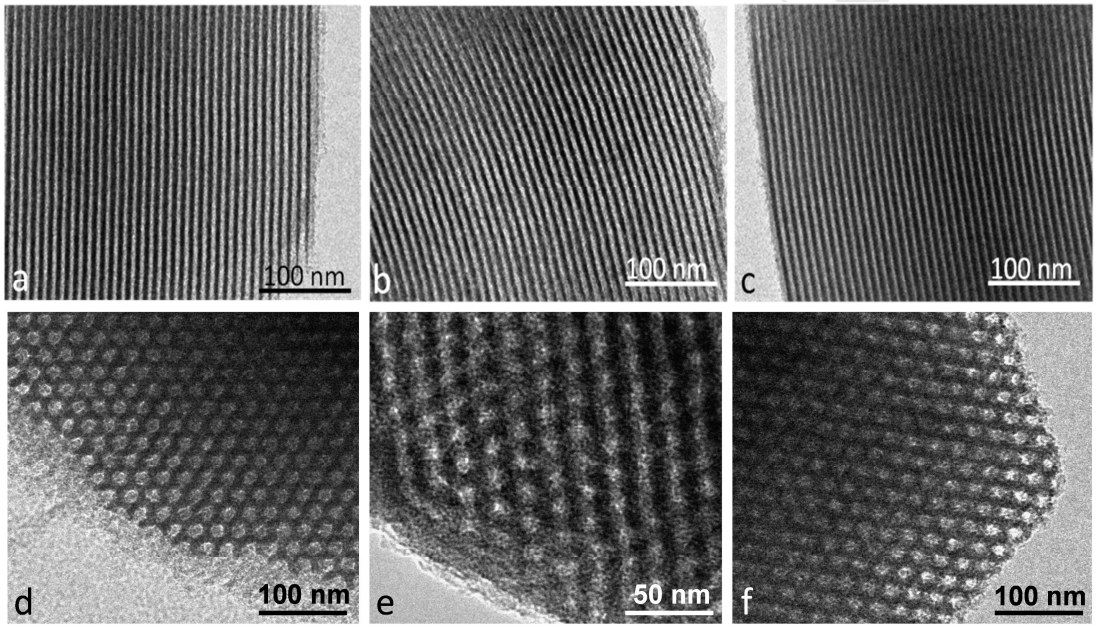

Figure S1. TEM images of SBA-15 (a, d), AP-SBA-15-C (b, e) and AP-SBA-15-G (c, f).

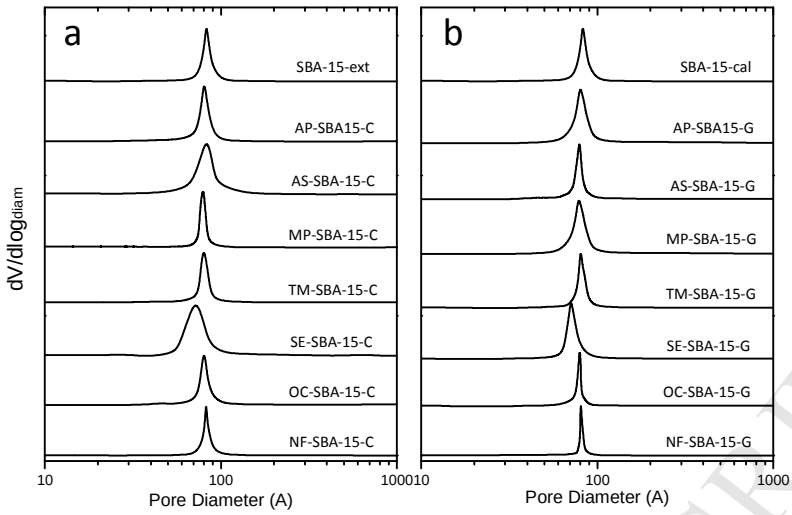

Figure S2. Pore size distribution for pure silica SBA-15-cal, SBA-15-ext material and functionalized samples synthesized by (a) co-condensation (b) grafting.

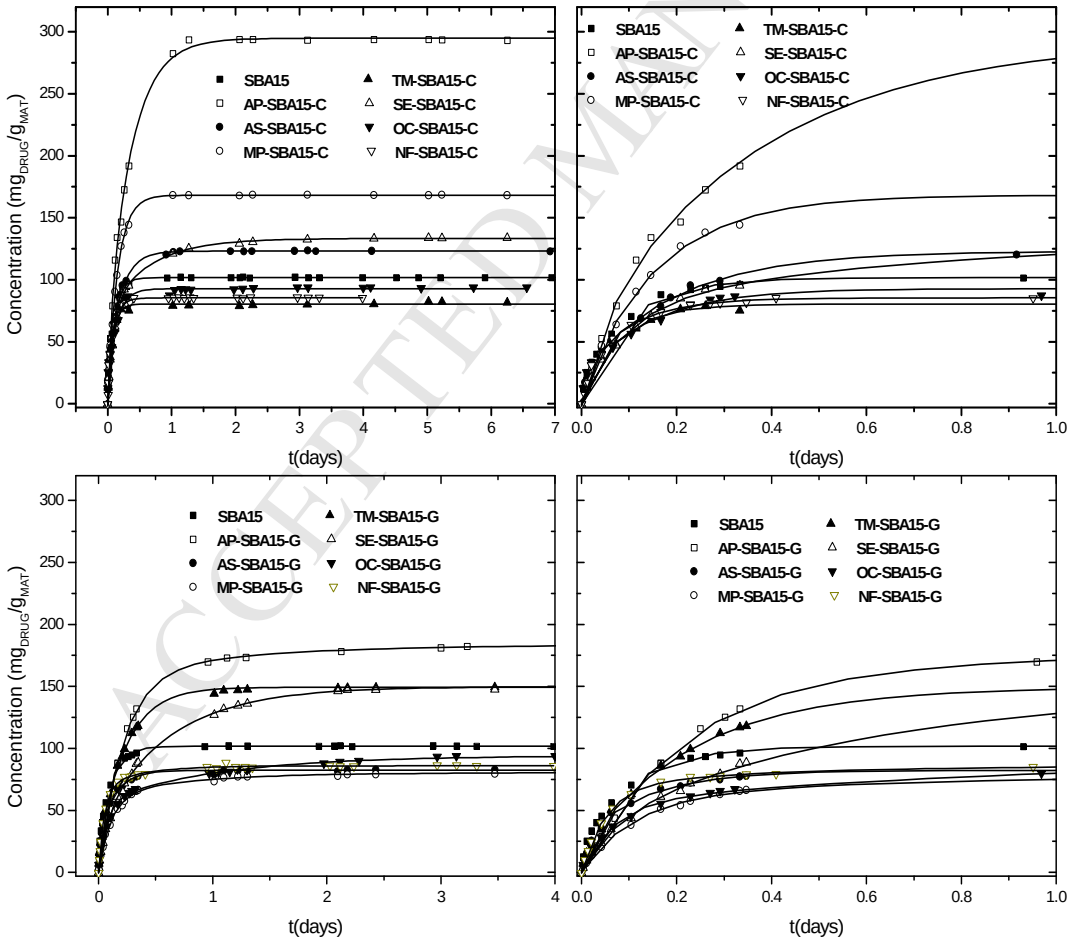

Figure S3. Drug delivery after 4 days in terms of concentration of methylprednisolone released from the silica SBA-15 sample and functionalized SBA-15 (by co-condensation and grafting) materials at pH 7.4 (left plots) and after one day of delivery (right plots).

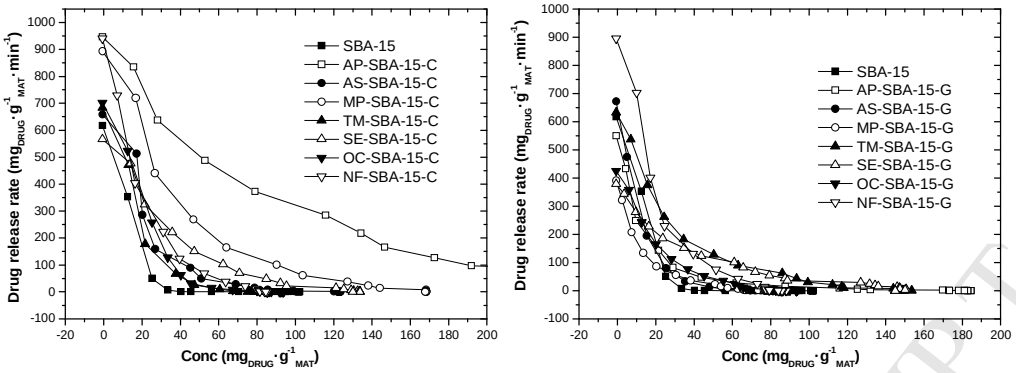

Figure S4. Instantaneous release rates of methylprednisolone from functionalized mesoporous SBA-15 silica obtained by co-condensation (C) and by grafting (G) into simulated body fluid (PBS buffer) at pH=7.4 and 37 ºC. The instantaneous release rate values represent the derivative of a given cumulative release profile at a specific point in time.

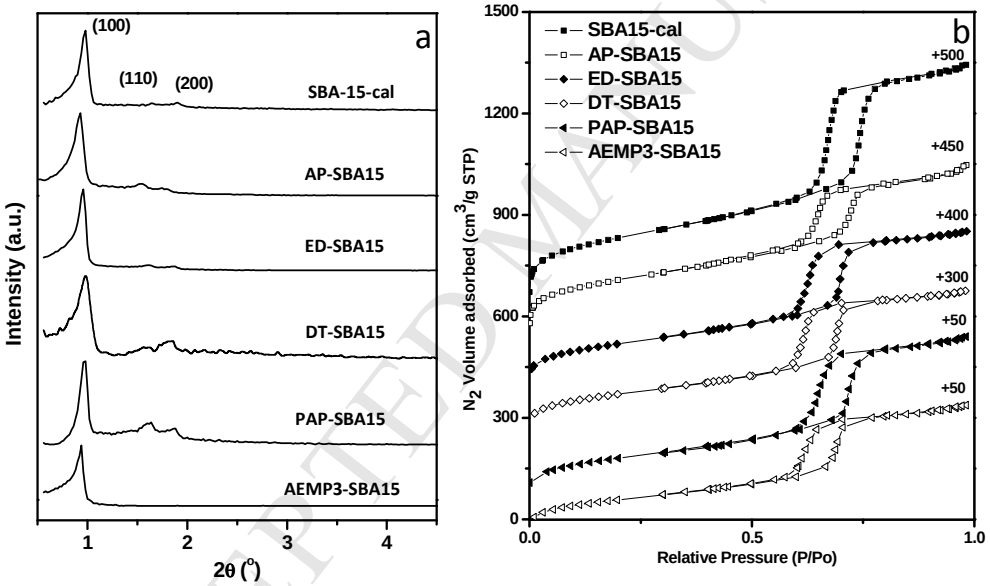

Figure S5 (a) X-ray diffraction patterns for SBA-15-cal and amino-functionalized SBA-15 materials synthesized by grafting **(b)** Nitrogen adsorption isotherms at 77 K for pure silica SBA-15-cal material and amino-functionalized samples synthesized by grafting.

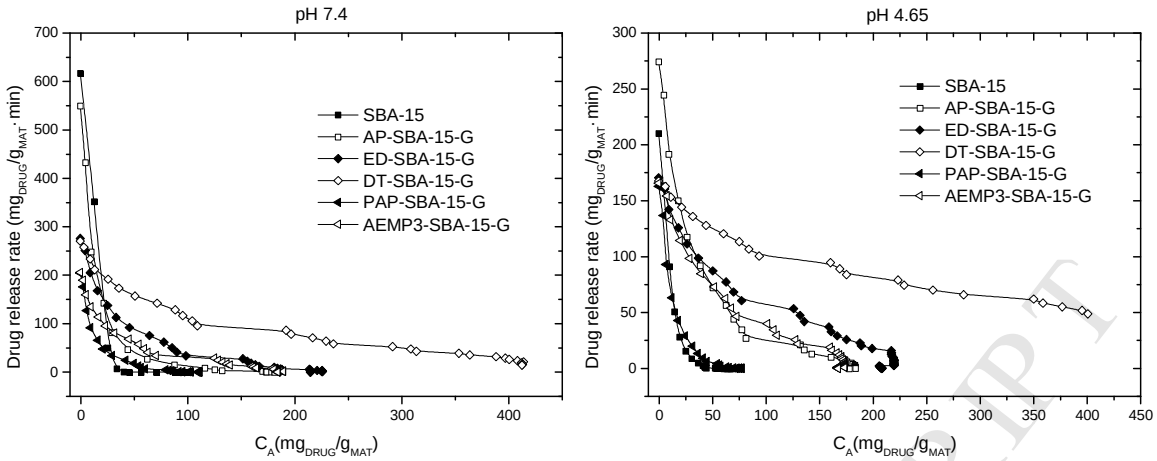

Figure S6. Instantaneous release rates of methylprednisolone from amino-functionalized mesoporous SBA-15-cal silica into simulated body fluid (PBS buffer) at pH=7.4 and 4.6 and 37 ºC. The instantaneous release rate values represent the derivative of a given cumulative release profile at a specific point in time.

Table S1. Fitting parameters obtained by mathematical fitting of the cumulative release profiles of methylprednisolone amino-functionalized mesoporous SBA-15 silica materials using first-order kinetic, and Korsmeyer-Peppas drug release models.

Material pH 7.4	Korsmeyer-Peppas $f(t) = K \cdot t^n$			First Order Kinetic $f(t) = f_{max} \cdot [1-\exp(-K \cdot t)]$		
	K	n	R^2	f_{max}	K	R^2
SBA-15-cal	206±7.77	0.47±0.01	0.997	101±0.71	13.8±0.68	0.985
AP-SBA-15-G	336±8.40	0.76±0.01	0.999	181±0.80	3.95±0.08	0.998
ED-SBA-15-G	163±4.93	0.53±0.02	0.986	215±4.15	1.42±0.11	0.973
DT-SBA-15-G	203±1.76	0.60±0.01	0.997	402±4.83	0.71±0.03	0.990
PAP-SBA-15-G	90±5.06	0.51±0.04	0.951	103±1.98	2.33±0.22	0.960
AEMP3-SBA-15-G	131±2.01	0.61±0.01	0.997	184±1.84	1.22±0.05	0.992

Material pH 4.65	Korsmeyer-Peppas $f(t) = K \cdot t^n$			First Order Kinetic $f(t) = f_{max} \cdot [1-\exp(-K \cdot t)]$		
	K	n	R^2	f_{max}	K	R^2
SBA-15-cal	73.8±2.84	0.42±0.02	0.987	66.6±1.73	4.17±0.59	0.880
AP-SBA-15-G	147±9.07	0.53±0.04	0.980	178±3.00	1.74±0.14	0.978
ED-SBA-15-G	125±1.97	0.52±0.02	0.995	208±4.30	0.9±0.02	0.965
DT-SBA-15-G	154±1.32	0.51±0.01	0.998	403±7.18	0.43±0.08	0.985
PAP-SBA-15-G	59.3±3.42	0.49±0.04	0.946	71.3±1.50	2.75±0.33	0.942
AEMP3-SBA-15-G	104±2.77	0.52±0.02	0.983	167±3.73	1.1±0.12	0.954

Surface-functionalization of mesoporous SBA-15 silica materials for controlled release of methylprednisolone sodium hemisuccinate: influence of functionality type and strategies of incorporation

J. Ortiz-Bustos, A. Martín, V. Morales, R. Sanz, and R. A. García-Muñoz

Chemical and Environmental Engineering Group, Universidad Rey Juan Carlos,

C/ Tulipán s/n, 28933 Móstoles, Madrid, Spain

Highlights

Mesoporous SBA-15 silica materials functionalized with several organic groups.

Loading and controlled drug release of the model corticoid methylprednisolone.

Influence of the type of organic moieties incorporated and synthesis procedure used.